BIOMOLECULES & THERAPEUTICS

Original Article
Biomol Ther 32(5), 568-576 (2024)

Domperidone, a Dopamine Receptor D2 Antagonist, Induces Apoptosis by Inhibiting the ERK/STAT3-Mediated Pathway in Human Colon Cancer HCT116 Cells

So Jin Sim[1,†], Jeong-Hoon Jang[2,†], Joon-Seok Choi[2] and Kyung-Soo Chun[1,*]

[1]*College of Pharmacy, Keimyung University, Daegu 42601,*
[2]*College of Pharmacy, Daegu Catholic University, Gyeongsan 38430, Republic of Korea*

Abstract

Colorectal cancer (CRC) continues to demonstrate high incidence and mortality rates, emphasizing that implementing strategic measures for prevention and treatment is crucial. Recently, the dopamine receptor D2 (DRD2), a G protein-coupled receptor, has been reported to play multiple roles in growth of tumor cells. This study investigated the anticancer potential of domperidone, a dopamine receptor D2 antagonist, in HCT116 human CRC cells. Domperidone demonstrated concentration- and time-dependent reductions in cell viability, thereby inducing apoptosis. The molecular mechanism revealed that domperidone modulated the mitochondrial pathway, decreasing mitochondrial Bcl-2 levels, elevating cytosolic cytochrome C expression, and triggering caspase-3, -7, and -9 cleavage. Domperidone decreased in formation of β-arrestin2/MEK complex, which contributing to inhibition of ERK activation. Additionally, treatment with domperidone diminished JAK2 and STAT3 activation. Treatment of U0126, the MEK inhibitor, resulted in reduced phosphorylation of MEK, ERK, and STAT3 without alteration of JAK2 activation, indicating that domperidone targeted both MEK-ERK-STAT3 and JAK2-STAT3 signaling pathways. Immunoblot analysis revealed that domperidone also downregulated DRD2 expression. Domperidone-induced reactive oxygen species (ROS) generation and *N*-acetylcysteine treatment mitigated ROS levels and restored cell viability. An *in vivo* xenograft study verified the significant antitumor effects of domperidone. These results emphasize the multifaceted anticancer effects of domperidone, highlighting its potential as a promising therapeutic agent for human CRC.

Key Words: Domperidone, Dopamine receptor D2, Reactive oxygen species, Colorectal cancer, STAT3, Apoptosis

INTRODUCTION

Colorectal cancer (CRC) is the third most prevalent cancer globally, in terms of incidence and mortality, with a concerning increase in morbidity and mortality rates (Biller and Schrag, 2021; Piao *et al*., 2022; Sahin *et al*., 2022; Alese *et al*., 2023). This escalating trend poses a significant public health threat worldwide. Following an initial diagnosis, 20% of patients with CRC progress to metastatic disease, and an additional 25% with initially localized disease subsequently experience metastasis (Biller and Schrag, 2021; Alese *et al*., 2023). Currently, surgical resection and chemoradiotherapy represent the primary treatment modalities, with surgery being the sole curative option. A notable recurrence rate persists despite radical surgery, and CRC demonstrated significant chemotherapy resistance (Alese *et al*., 2023). Consequently, innovative and more effective approaches in the current management of CRC are urgently required.

The MAP kinase signaling pathway, comprising the ERK, JNK, and p38 cascades, plays a pivotal role in regulating various cellular processes, including proliferation, differentiation, and apoptosis (Dhillon *et al*., 2007; Braicu *et al*., 2019). MAP kinase pathway dysregulation has been associated with CRC initiation and progression (Fang and Richardson, 2005; Dhillon *et al*., 2007; Ponsioen *et al*., 2021). Genetic alterations, such as mutations in KRAS and BRAF, frequently activate this pathway, thereby contributing to uncontrolled cell growth and apoptosis evasion (Midthun *et al*., 2019). Elucidating the intricate interplay within the MAP kinase signaling cascade in the context of CRC is crucial for determining novel therapeutic targets and advancing precision medicine approaches. JAK2-STAT3 signaling plays a crucial role in CRC progression, in

Open Access **https://doi.org/10.4062/biomolther.2024.048**

Received Mar 20, 2024 **Revised** Apr 11, 2024 **Accepted** Apr 22, 2024
Published Online Jun 25, 2024

***Corresponding Author**
E-mail: chunks@kmu.ac.kr
Tel: +82-53-580-6647
[†]The first two authors contributed equally to this work.

addition to MAP kinase signaling (Mengie Ayele *et al*., 2022). Notably, STAT3 demonstrates a distinct characteristic in CRC, considering that the interleukin-6/STAT3 signaling axis plays a pivotal role as a key inflammatory mechanism in colitis-associated cancer (Mengie Ayele *et al*., 2022). Moreover, STAT3 is markedly activated in CRC, amplifying cancer cell proliferation, tumor growth, invasion, and migration (Gargalionis *et al*., 2021). These attributes emphasize STAT3's potential as a promising target for therapeutic intervention.

Dopamine, a widely recognized neurotransmitter associated with diverse brain functions, such as rewards and motivation, has attracted attention in medical studies (Dalton *et al*., 2005). Intriguingly, research indicates a lower cancer incidence in patients with schizophrenia treated with dopamine receptor antagonists and a reduced susceptibility to most cancers in individuals with Parkinson's disease (Driver *et al*., 2007). These observations indicate the presence of dopamine receptors in peripheral tissues, and blocking these receptors may help decrease cancer risk. Notably, psychotropic drug screening identified phenothiazines to have anticancer properties as early as 1978 (Barone, 1999).

Dopamine receptor D2 (DRD2), a specific dopamine receptor subtype, is upregulated in various cancers (Mu *et al*., 2017; Gholipour *et al*., 2018; Pierce *et al*., 2021; Shakya *et al*., 2023). Upon dopamine binding to DRD2, β-arrestin plays a crucial role in desensitizing and internalizing activated DRD2 and regulating downstream signaling. This pathway, particularly relevant in cancer because of DRD2 upregulation in various cancers, provides insights into the dynamic modulation of dopamine signaling and its potential impact on cancer-related processes, including cancer initiation, promotion, progression, and metastasis (Mu *et al*., 2017; Gholipour *et al*., 2018; Pierce *et al*., 2021; Shakya *et al*., 2023).

This study explored the effect of domperidone on the apoptosis of HCT116 CRC cells, focusing on the DRD2-MAPK and STAT3 signaling pathways.

MATERIALS AND METHODS

Cell cultures

The American Type Culture Collection (Manassas, VA, USA) provided HCT116, a human colorectal carcinoma cell line, maintained in Dulbecco's Modified Eagle Medium supplemented with 10% (v/v) fetal bovine serum and 1% (v/v) penicillin–streptomycin at 37°C in a humidified incubator with 5% CO_2 and 95% air.

Reagents

Hyclone Laboratories (Logan, UT, USA) provided all cell culture reagents. Sigma-Aldrich (St. Louis, MO, USA) supplied *N*-acetylcysteine (NAC) and the primary antibody against β-actin. Cell Signaling Technology, Inc. (Beverly, MA, USA) supplied primary antibodies specific for cleaved caspase-9, caspase-7, caspase-3, cleaved PARP, cytochrome C, p-STAT3 (S727), p-STAT3 (Y705), STAT3, p-JAK2, JAK2, and cyclin D1. Santa Cruz Biotechnology (Dallas, TX, USA) provided antibodies against cyclin D1, D2, and D3. Novus Biologicals (Littleton, CO, USA) and Abcam (Cambridge, UK) supplied antisurvivin and anti-COX IV antibodies, respectively. Cell Signaling Technology, Inc. provided secondary antibodies conjugated with horseradish peroxidase. Invitrogen (Carlsbad, CA, USA) supplied 2',7'-dichlorofluorescin diacetate (DCF-DA). Thermo Fisher Scientific (Waltham, MA, USA) provided Hank's balanced salt solution (HBSS).

Cell viability assay

Cell viability was identified as previously described (Kundu *et al*., 2014). Briefly, 2×10^3 cells per well were seeded in triplicate into a 96-well plate. Cells were exposed to different domperidone concentrations for the indicated times in 0.1 ml of media. A 20 μL (3-[4, 5-dimethylthiazol-2-yl]-5-[3-carboxymethoxyphenyl]-2-[4-sulfophenyl]-2H-tetrazolium) solution (MTS reagent; Promega, Madison, WI, USA) was then added and incubated for 1 h at 37°C in the dark. Finally, a Versamax microplate reader (Molecular Devices, San Jose, CA, USA) was used to identify cell viability by measuring absorbance at 490 nm.

Annexin V/propidium iodide (PI) staining assay

A fluorescein isothiocyanate-annexin V staining kit (BD Biosciences, San Jose, CA, USA) was used to identify the percentage of dead cells, following the manufacturer's instructions. In brief, the cells were treated with domperidone as indicated in the figure legends. The cells were harvested and washed with phosphate buffer saline (PBS), followed by resuspension in binding buffer containing Annexin V and PI. Finally, flow cytometry (BD Biosciences) was used to determine the percentage of dead cells.

Assessment of intracellular reactive oxygen species (ROS) levels

Intracellular ROS levels were measured using DCF-DA fluorescence as described previously (Raut *et al*., 2021). In brief, the cells were stimulated with domperidone as indicated in the figure legends. The cells were washed with HBSS, followed by incubation with DCF-DA of 25 μM for 30 min in the dark at 37°C. The cells were further washed with HBSS to remove excess DCF-DA, and either fluorescence microscopy or flow cytometry was used to identify intracellular ROS levels. An excitation wavelength of 480 nm and an emission wavelength of 525 nm by flow cytometry was used to evaluate the fluorescence intensity of oxidized DCF.

Isolation of mitochondrial and cytoplasmic proteins

Cytoplasmic and mitochondrial protein fractions were obtained after treating HCT116 cells with domperidone using the Mitochondria/Cytosol Fractionation Kit (BioVision Inc., Milpitas, CA, USA) following the manufacturer's instructions (Raut *et al*., 2021). Briefly, 2×10^6 cells were collected after domperidone treatment as indicated in the figure legends. The cells were washed with ice-cold PBS and centrifuged at 600 g for 5 min at 4°C. The cells were resuspended in cytosolic buffer and incubated on ice for 10 min. The homogenate was obtained by passing the cell suspension through a Dounce homogenizer. The homogenate was centrifuged at 700 g for 10 min at 4°C, and the supernatant was further centrifuged at 10,000 g for 30 min at 4°C. The supernatant was considered to be the cytosolic fraction. The pellet was resuspended in a mitochondrial extraction buffer mix and vortexed for 10 s to prepare the mitochondrial fraction. Western blot analysis was used to identify the cytochrome C and Bcl-2 levels in the cytoplasm and mitochondria.

Immunoblot assay

Cells were harvested and lysed using RIPA lysis buffer to obtain total cell lysates to identify the protein expression of target genes. A bicinchoninic acid protein assay kit (Pierce Biotechnology, Rockford, IL, USA) was used to further quantify the lysates. A total cellular protein of 30-50 μg was resolved on 8-15% SDS-PAGE gels and transferred to polyvinylidene difluoride (PVDF) membranes for western blot analysis. The membranes were blocked with 5% (w/v) skim milk for 1 h and then incubated with primary antibodies (1:1,000 dilutions prepared in TBS containing 0.1% Tween 20) overnight at 4°C. After washing with TBST, the membranes were incubated with appropriate secondary antibodies conjugated with horseradish peroxidase (1:5,000) for 1 h. Hypersignal WesternBright ECL HRP substrate (Advansta, San Jose, CA, USA) or Supersignal™ West Femto maximum sensitivity substrate (Thermo Fisher Scientific) was used to develop the membranes. following the manufacturer's instructions. Finally, ImageQuant™ LAS 4000 (Fujifilm Life Science, Tokyo, Japan) was used to capture chemiluminescence images of the membranes.

Transient transfection with small interfering RNA (siRNA)

Cells were seeded at a density of 5×10^5 cells/100 mm dish. After overnight incubation, the cells were transfected with siRNA targeting STAT3 or control scrambled using Oligofectamine™ transfection reagent (Thermo Fisher Scientific) following the manufacturer's instructions. Western blot analysis after 36 h of transfection was used to determine gene silencing efficiency. This study obtained siRNA duplexes used from Bioneer (Daejeon, Korea). The nucleotide sequences of the STAT3 siRNA duplexes were 5′-UGUUCUCUGAGACCCAUGA-3′ (forward primer) and 5′-UCAUGGGUCUCAGAGAACA-3′ (reverse primer).

Luciferase reporter gene assay

A dual-luciferase reporter assay system (Promega) was used for the luciferase reporter assay for STAT3, as described previously (Raut and Park, 2020). Briefly, HCT116 cells were seeded at a density of 3×10^5 cells/well onto a six-well plate. After overnight incubation, cells were cotransfected with STAT3 and Renilla luciferase plasmids using FuGENE HD transfection reagent (Promega) for 24 h, following the manufacturer's instructions. The cells were further stimulated with the indicated domperidone concentrations for 24 h. The cells were lysed with passive lysis buffer and centrifuged at 13,000 rpm for 10 min to obtain a whole-cell lysate. Finally, the luminescence of firefly and renilla was identified by adding luciferase assay reagent and Stop & Glo reagent, respectively, in 20 μL of cell lysate using a multimode microplate reader (Tecan, Mannedorf, Switzerland). The values are expressed relative to the controls after normalization with renilla luciferase because the renilla luciferase plasmid acts as an internal loading control for transfection efficiency.

Immunoprecipitations

Supernatants were incubated for 1 h with gentle rocking at 4°C by adding 1.0 μg of the appropriate control IgG (corresponding to the host species of the primary antibody) and 20 μL of the corresponding suspended protein A/G-agarose (Santa Cruz Biotechnology) to eliminate nonspecific binding in tissue lysates. After centrifugation at 1,000 g for 30 s at 4°C, the supernatants containing protein of 200 μg were transferred to a microcentrifuge tube, and a primary antibody of 1.0 μg was added, followed by incubation for 2 h at 4°C. Protein A/G-agarose of 20 μL was then added and incubated at 4°C overnight with rotation. The immunoprecipitates were collected by centrifugation at 1,000×g for 30 s at 4°C, and the pellet was gently washed four times with a cell lysis buffer of 1.0 ml. After the final wash, the supernatants were discarded, and the pellets were reconstituted in electrophoresis sample buffer for subsequent loading.

Development of HCT116 tumor xenograft

All animal experiments were performed following the guidelines of the Keimyung University Institutional Animal Care and Use Committee (KM2021-016). HCT116 tumor xenografts were prepared using 5-week-old (weight: 20-25 g) BALB/c nude mice (Orient Bio, Inc., Seongnam, Korea). HCT116 cells (2×10^6) suspended in PBS–Matrigel of 200 μL (in a 1:1 ratio) were injected into the right flank of BALB/c nude mice. The mice were randomly divided into the following three groups (n=5 for each group) when the tumor size reached approximately 150 mm^3 in volume (10 days after cell injection): control (received corn oil) and domperidone treatment at 4 and 20 mg/kg. Domperidone was intraperitoneally administered five times a week 22 days after cell injection during the treatment period (3 weeks). Similarly, tumor volume was assessed twice a week during treatment, and tumor volume was calculated using the following formula: $V=(width)^2\times length/2$.

Statistical analysis

Data are presented as the mean ± standard deviation of at least three independent experiments. Paired Student's *t*-test or analysis of variance was used for statistical analysis. A p value <0.05 was considered statistically significant.

RESULTS

Domperidone induces apoptosis in HCT 116 CRC cells

An MTS assay was conducted to assess the association of domperidone with HCT116 cell viability, which revealed a significant concentration- and time-dependent reduction in cell viability (Fig. 1A, 1B). HCT116 cell treatment with domperidone of 50 μM for 72 h inhibited growth by nearly 90% compared with control cells. The IC_{50} values for cell growth inhibition were 34.57 μM at 48 h for HCT116 cells. Fluorescence-activated cell sorting (FACS) was performed to detect the apoptotic cell population by double staining with Annexin V and PI to further determine the possible role of apoptosis in cell death by domperidone. FACS analysis following Annexin V/PI staining demonstrated an increase in apoptotic cells from 3.78% to 48.67% with ascending concentrations of domperidone (5-25 and 50 μM) in HCT116 cells, indicating its potential anticancer effects (Fig. 1C, 1D).

Domperidone exerts apoptosis via the mitochondrial pathway

The intrinsic apoptotic pathway, or mitochondrial pathway, involves the release of cytochrome C from the mitochondria triggered by outer mitochondrial membrane permeabilization mediated by Bcl-2 (Wang and Youle, 2009). We examined Bcl-2 protein levels by immunoblotting to assess whether domperidone-induced apoptosis involves this pathway. Dom-

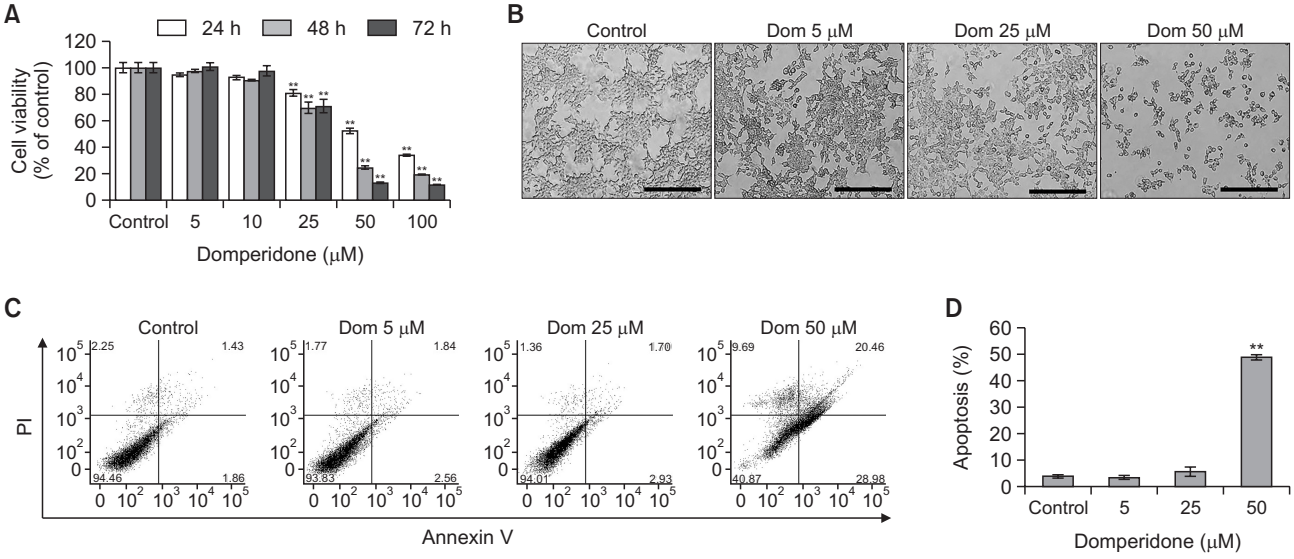

Fig. 1. Antiproliferative effect of domperidone on HCT116 cells. (A) HCT116 cells were treated with domperidone (0, 5, 10, 25, 50, and 100 μM) for 24, 48, and 72 h, and cell viability was determined using the MTS cell viability assay. Data are shown as the mean ± standard deviation (SD), (n=3). (B) Representative images of domperidone-treated HCT116 cells. The scale bar indicates 200 μm. (C, D) HCT116 cells treated with varying domperidone concentrations (0, 5, 10, 25, and 50 μM) for 48 h were analyzed by FACS with Annexin V/PI staining. Data are shown as the mean ± SD, (n=3). ***p*<0.01.

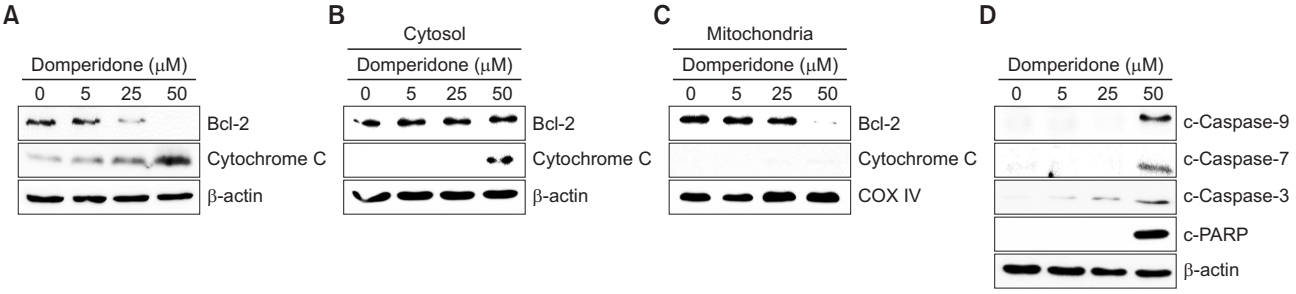

Fig. 2. Disturbance of the antiapoptotic Bcl-2 protein by domperidone. (A) Immunoblot analysis of mitochondrial apoptosis-related proteins Bcl-2 and cytochrome C. (B) Immunoblot analysis of mitochondrial apoptosis-related proteins cytosolic Bcl-2 and cytochrome C in HCT116 cells. (C) Immunoblot analysis of mitochondrial apoptosis-related proteins Bcl-2 and cytochrome C in the mitochondrial fraction of HCT116 cells and COX IV was used as the loading control. (D) The levels of cleaved forms of caspase-3, -7, and -9 and PARP monitored by immunoblot. β-Actin was used as the loading control.

peridone treatment decreased Bcl-2 levels while increasing cytochrome C expression in whole-cell lysates (Fig. 2A). Subsequent mitochondrial fractionation confirmed a reduction in mitochondrial Bcl-2 expression and an elevation of cytosolic cytochrome C, indicating cytochrome C translocation from mitochondria to the cytosol by domperidone (Fig. 2B, 2C). Additionally, caspase-3, -7, and -9 cleavage and PARP protein fragmentation, observed through immunoblot analysis, indicated domperidone-induced cell death through the mitochondrial apoptotic pathway (Fig. 2D). These results indicate that domperidone triggered apoptosis in HCT116 cells by modulating the mitochondrial apoptotic pathway.

Domperidone suppresses the MAP kinase signaling pathway

We investigated the effect of domperidone on MAP kinase signaling activation because of its potential role in regulating cell survival and apoptosis to elucidate the molecular mechanism underlying the cytotoxic effect of domperidone in HCT116 cells (Fang and Richardson, 2005; Dhillon *et al*., 2007; Oh *et al*., 2018). Domperidone treatment significantly inhibited MEK and ERK phosphorylation, with no effect on their total protein levels (Fig. 3A). We tested JAK2/STAT3 signaling, which is recognized for its involvement in cell survival and apoptosis pathways in the context of cancer cell death, in addition to MAP kinase signaling (Kundu *et al*., 2014; Mengie Ayele *et al*., 2022; Park *et al*., 2022). STAT3 levels remained relatively unchanged. However, we observed that STAT3 phosphorylation on Ser727 and Tyr705 decreased upon domperidone treatment (Fig. 3A). We evaluated the JAK2 level, an upstream kinase of STAT3. The phosphorylated form of JAK2 was significantly suppressed, whereas the JAK2 level remained constant after domperidone exposure (Fig. 3A). Moreover, we validated the inhibitory effect of domperidone on STAT3 activ-

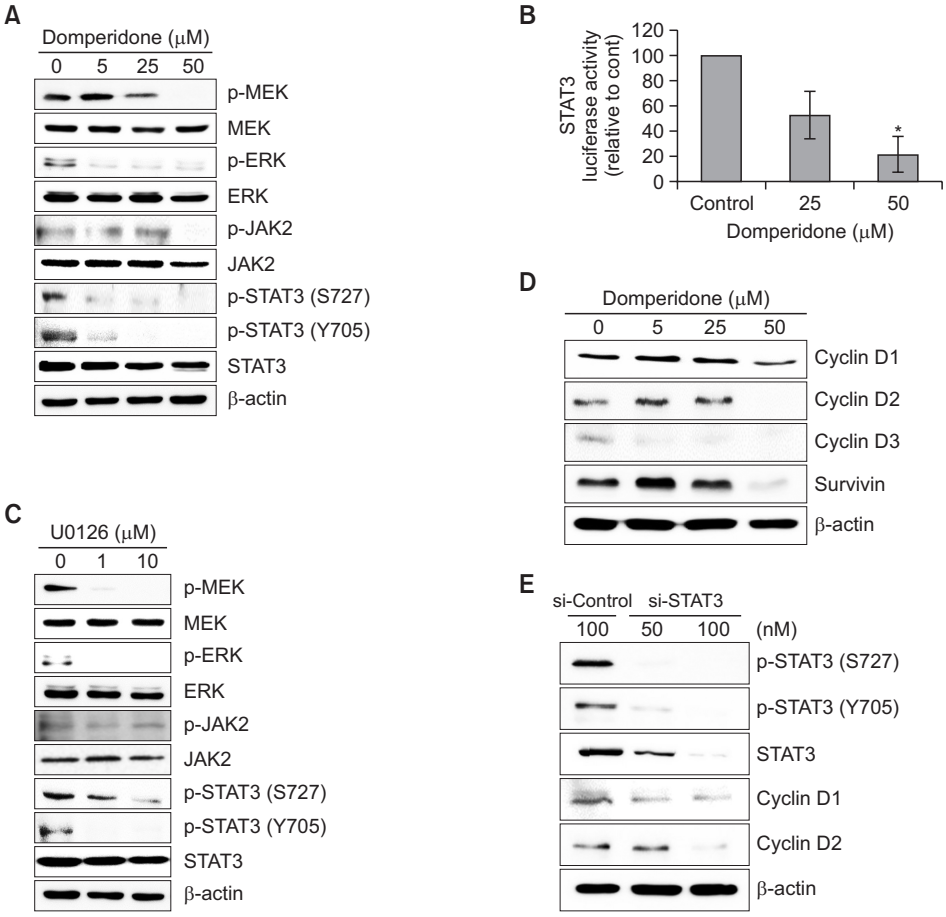

Fig. 3. Regulation of the MEK/ERK signaling pathway by domperidone. (A) Immunoblot analysis of proteins involved in the ERK and STAT3 signaling pathways. (B) STAT3 reporter gene activity in response to domperidone. Values are presented as the mean ± standard deviation (SD), (n=3). (C) Immunoblot analysis of proteins involved in the ERK and STAT3 signaling pathways in response to the selective MEK inhibitor U0126. (D) Immunoblot analysis of cell cycle-related proteins cyclin D1, D2, D3, and survivin. (E) HCT116 cells were transfected with siRNA targeting STAT3 or scrambled control siRNA for 36 h. Immunoblot analysis of STAT3, cyclin D1, and D2. β-Actin was used as the loading control. **p*<0.05.

ity using the STAT3 reporter gene assay (Fig. 3B). ERK1/2 regulates STAT3 expression in oral cancer, indicating crosstalk between the MAP kinase and STAT3 pathway (Gkouveris *et al*., 2014). We used the pharmacological MEK inhibitor U0126 to verify the crosstalk. Consistent with oral cancer findings, U0126 treatment reduced MEK, ERK, and STAT3 phosphorylation, thereby confirming the crosstalk between MAP kinase signaling and STAT3. However, no significant alterations were observed in JAK2 phosphorylation in U0126-treated HCT116 cells, indicating that domperidone targeted both MEK-ERK-STAT3 and JAK2-STAT3 signaling pathways (Fig. 3C). Additionally, we identified the effect of domperidone on STAT3-dependent genes, including cyclin and survivin. Domperidone significantly abrogated the expression of cyclin D1, D2, and D3 and survivin in HCT116 cells (Fig. 3D). Transient silence of STAT3 further confirmed the connection between STAT3 signaling and cyclin D1 and D2 expression (Fig. 3E). These results reveal that the cytotoxic effect of domperidone in HCT116 cells involves significant the MEK/ERK/STAT3 signaling pathway inhibition.

Domperidone downregulates the DRD2-mediated signaling pathway

We observed a significant reduction in protein levels of DRD2 in HCT116 cells through immunoblot analysis to investigate the impact of domperidone on dopamine receptor D series expression (Fig. 4A). DRD2, known to be overexpressed in various cancer types, engages downstream effectors, including the MAPK pathway, influencing cellular processes, such as proliferation, angiogenesis, and apoptosis (Mu *et al*., 2017; Gholipour *et al*., 2018; Pierce *et al*., 2021). Recent studies revealed that GPCR ligand stimulation induced the formation of a GPCR-β-arrestin-MEK complex and MEK activation (Qu *et al*., 2021; Kim *et al*., 2022; Kahsai *et al*., 2023). The Western blot data in Fig. 4B and 4C show that domperidone treatment reduced the β-arrestin2-MEK complex levels, as evidenced by immunoprecipitation with antibodies to β-arrestin2 and MEK, respectively. Additionally, the data indicate that domperidone treatment did not influence the β-arrestin2 or MEK levels individually. Thus, the data indicate that DRD2 suppression by domperidone reduced β-arrestin2-MEK complex formation in HCT116 cells. These results indicate selective modulation of

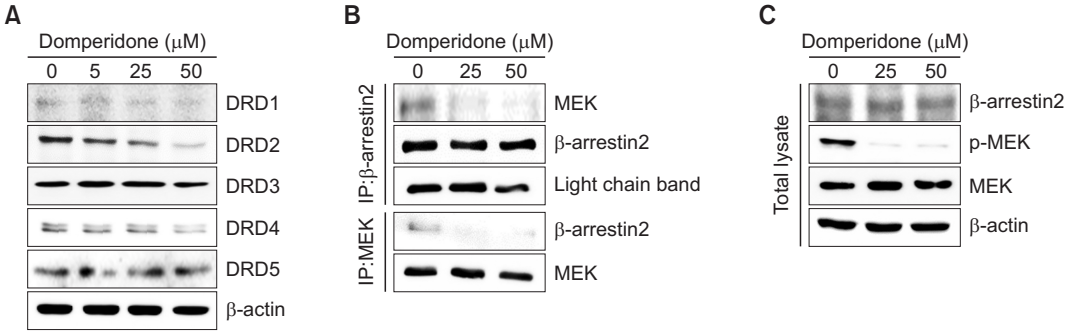

Fig. 4. DRD2-mediated signaling pathway downregulation by domperidone. HCT116 cells were treated with domperidone (0, 5, 25, and 50 μM) for 24 h. (A) Immunoblot analysis of the dopamine receptors DRD1 through DRD5. (B) Co-immunoprecipitation of β-arrestin 2 and MEK. (C) Immunoblot analysis of β-arrestin 2 and MEK.

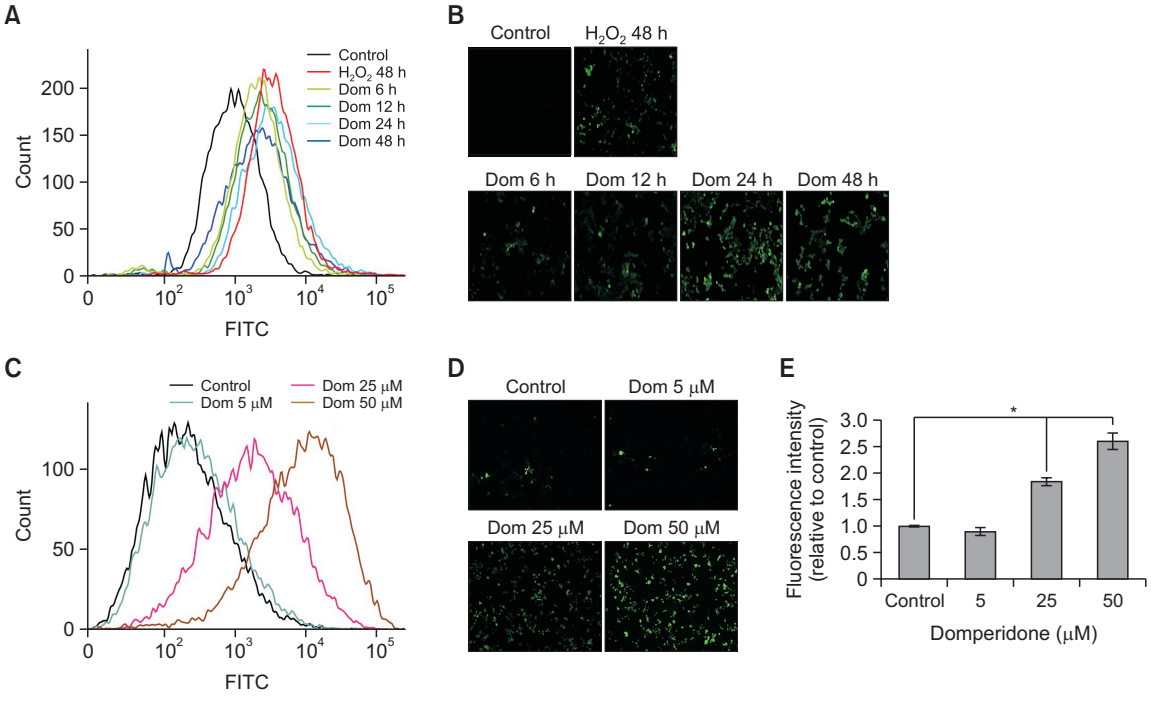

Fig. 5. Induction of ROS generation by domperidone in HCT116 cells. HCT116 cells were stimulated with domperidone (0, 5, 25, and 50 μM) for 6, 12, 24, and 48 h. The intracellular accumulation of ROS was identified by measuring the fluorescence of DCF-DA using FACS and fluorescence microscopy. (A, C) Histogram of DCF fluorescence. (B, D) DCF fluorescence microscopic images. (E) Graph of DCF fluorescence intensity. Data are shown as the mean ± standard deviation (SD), (n=3). *p<0.05.

the DRD2-β-arrestin2-MEK signaling cascade by domperidone in HCT116 cells.

Domperidone-induced ROS generation in HCT116 cells

Excessive ROS accumulation by several anticancer agents exerts anticancer activities (Perillo *et al*., 2020; Richa *et al*., 2020). The investigation of the association between ROS generation and apoptosis by domperidone revealed a time- and concentration-dependent increase in ROS production within HCT116 cells upon domperidone exposure (Fig. 5A-5E). HCT116 cell treatment with NAC caused a notable reduction in domperidone-induced ROS generation (Fig. 6A, 6B). Additionally, the decrease in cell viability caused by domperidone was restored upon NAC treatment (Fig. 6C). These results indicate that domperidone influences ROS accumulation, potentially implicating it in cellular processes, including apoptosis, in HCT116 cells.

Domperidone demonstrates antitumor effects in an *in vivo* xenograft model

The antitumor properties of domperidone were further investigated in HCT116 tumor xenografts developed in BALB/c nude mice. Domperidone treatment at 4 and 20 mg/kg concentrations demonstrated a remarkable reduction in tumor cell growth in an *in vivo* xenograft model compared with the control group without changing body weight, highlighting its pronounced antitumor effects *in vivo* (Fig. 7A-7C).

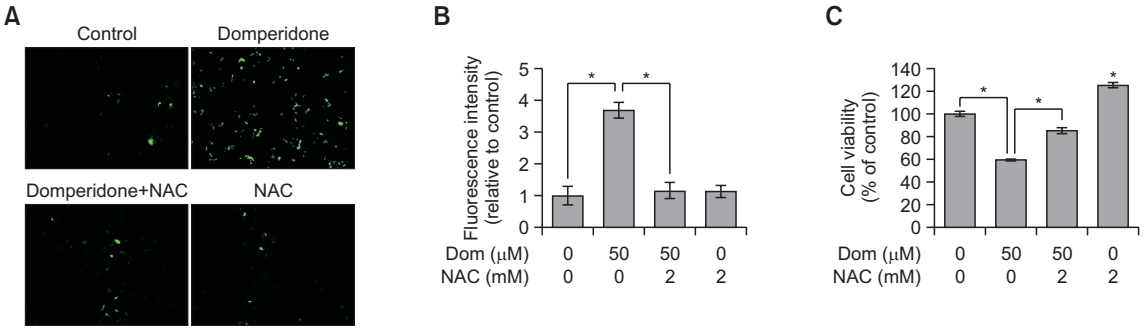

Fig. 6. Effect of NAC on domperidone-induced ROS generation and cell death in HCT116 cells. HCT116 cells were treated with the ROS scavenger NAC (5 mM) for 1 h, before preincubation with domperidone (50 μM) for 48 h. (A) DCF-DA fluorescence microscopic images. (B) Graph of DCF-DA fluorescence intensity. Data are shown as the mean ± standard deviation (SD), (n=3). (C) Cell viability was measured by the MTS cell viability assay. Data are shown as the mean ± standard deviation (SD), (n=3). *p<0.05.

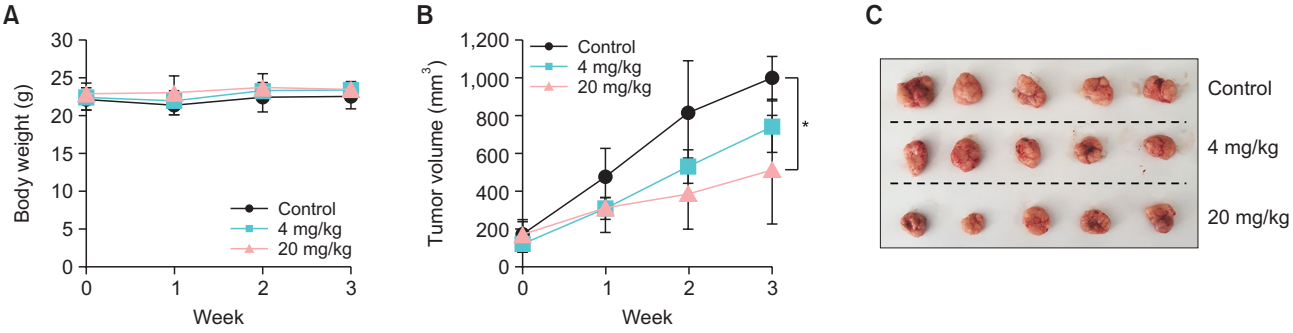

Fig. 7. Inhibitory effect of domperidone on *in vivo* xenograft tumor growth using HCT116 cells. Tumor xenografts of HCT116 cells were developed by injecting HCT116 cells mixed with Matrigel into the right flank of BALB/c nude mice (n=5 for each group). (A) Body weight change of mice during domperidone treatment. (B) HCT116 tumor growth in response to domperidone treatment. (C) Photograph of HCT116 xenograft tumors. Data are shown as the mean ± standard deviation (SD). *p<0.05.

DISCUSSION

This study investigated the association of domperidone with HCT116 CRC cells, revealing compelling insights into its cytotoxic and antitumor effects. Our results revealed that domperidone induced apoptosis in HCT116 cells, as evidenced by a significant concentration- and time-dependent reduction in cell viability, accompanied by an increase in apoptotic cells. These results are congruent with previous studies indicating the potential anticancer effects of domperidone (Shakya *et al*., 2023).

One key aspect explored in this study was the mitochondrial apoptotic pathway modulation by domperidone. Our results indicated a decrease in antiapoptotic Bcl-2 proteins, causing the release of cytochrome C and subsequent activation of caspase-3, -7, and -9, as well as PARP cleavage. The observed mitochondrial fractionation results further supported the notion of domperidone-induced apoptosis through the intrinsic apoptotic pathway (Wang and Youle, 2009; Jan and Chaudhry, 2019). These results contribute to a deeper understanding of the molecular mechanisms underlying domperidone-induced HCT116 cell death.

Moreover, we investigated the association of domperidone with the ERK signaling pathway, elucidating its multifaceted effects. Domperidone and U0126, a pharmacological MEK inhibitor, treatment caused substantial suppression of MEK, ERK, and STAT3 phosphorylation, indicating potential crosstalk between ERK and STAT3 signaling. Notably, our results indicate that ERK modulates STAT3 phosphorylation in cancer cells. In line with our results, previous studies reported a reduction in STAT3 phosphorylation at serine residues and a subsequent decrease in cyclin D1 expression when ERK1/2 was inhibited in OSCC cells (Gkouveris *et al*., 2014). The observed downregulation of key cell cycle regulators, including cyclin D1, D2, and survivin, further emphasizes the involvement of the ERK/STAT3 signaling pathway in mediating the cytotoxic effects of domperidone. ERK and STAT3 signaling dual inhibition by domperidone highlight its potential as a potent anticancer agent, considering the critical roles that these signaling pathways play in cancer cell growth. This dual-targeting property positions domperidone as a promising candidate for further investigation in cancer therapy.

Our investigation of the dopamine receptor signaling cascade revealed that domperidone selectively downregulated DRD2 protein levels in HCT116 cells. This specific modulation of the DRD2-β-arrestin2-MEK signaling cascade by domperidone indicates a potential avenue for its antitumor effects. Initially, we anticipated that domperidone would act as a DRD2 antagonist due to the observed reduction in MEK and ERK phosphorylation. However, our subsequent confirmation of DRD2 expression revealed that the antitumor effects of domperidone stem from a decrease in DRD2 expression rather

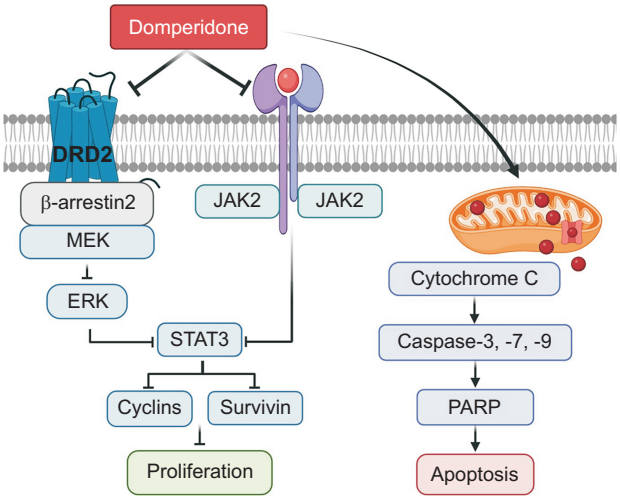

Fig. 8. A scheme of the molecular mechanisms underlying HCT116 cell apoptosis induction by ERK/STAT3 signaling pathway and ROS accumulation suppression.

than from an antagonistic effect. This implies that domperidone directly modulates the expression, prompting the need for further investigation into the underlying mechanisms governing its regulatory effects on DRD2. Additionally, our experiments with dopamine, the ligand for DRD2, failed to induce increased cell proliferation in HCT116 cells (Supplementary Fig. 1). Importantly, dopamine treatment did not restore the diminished cell proliferation attributed to the decreased DRD2 expression by domperidone (Supplementary Fig. 1). These combined results contribute to a more comprehensive understanding of the molecular targets and pathways affected by domperidone in CRC cells, emphasizing the intricate interplay between domperidone, DRD2, and the broader signaling cascade, prompting additional investigation of its potential therapeutic applications in cancer treatment.

A similar study focusing on the antitumor effect of domperidone in triple-negative breast cancer (TNBC) cells has recently been reported (Shakya *et al*., 2023). Similarly, domperidone-induced mitochondrial ROS generation led to apoptosis in TNBC cells. While the previous study emphasized the unchanged expression of MAPK signaling molecules and the inhibition of phosphorylation of JAK2, STAT1, and STAT3, our research elucidated the inhibition of ERK activation through domperidone-mediated decreased formation of the β-arrestin2/MEK complex and JAK2-STAT3 signaling, respectively. Moreover, in addition to the direct inhibition of the JAK2-STAT3 signaling pathway by domperidone, we revealed STAT3 signaling inhibition through ERK-STAT3 crosstalk in human CRC cells.

Additionally, our investigation into the association between ROS generation and apoptosis revealed that domperidone induced a concentration- and time-dependent increase in ROS production. NAC treatment attenuated domperidone-induced ROS generation and restored cell viability, indicating a potential role of ROS in cellular processes, including apoptosis, triggered by domperidone.

In conclusion, our comprehensive study provides evidence supporting domperidone as a potential therapeutic agent for CRC (Fig. 8). The induction of apoptosis, modulation of mitochondrial and ERK signaling pathways, downregulation of dopamine receptors, and *in vivo* antitumor effects collectively contribute to a better understanding of the molecular mechanisms underlying the cytotoxic effects of domperidone in HCT116 cells. Further investigations and clinical studies are warranted to confirm the translational viability of domperidone as a therapeutic option for CRC.

CONFLICT OF INTEREST

The authors report no declarations of interest. The authors alone are responsible for the content and writing of the paper.

ACKNOWLEDGMENTS

This study was supported by the Basic Science Research Program grant (No. 2020R1I1A3066367 to KSC; No. 2018R1D1A1A02050495 and 2021R1A2C1014399 to JSC) from the National Research Foundation (NRF) of the Republic of Korea.

REFERENCES

Alese, O. B., Wu, C., Chapin, W. J., Ulanja, M. B., Zheng-Lin, B., Amankwah, M. and Eads, J. (2023) Update on Emerging therapies for advanced colorectal cancer. *Am. Soc. Clin. Oncol. Educ. Book* **43**, e389574.

Barone, J. A. (1999) Domperidone: a peripherally acting dopamine2-receptor antagonist. *Ann. Pharmacother.* **33**, 429-440.

Biller, L. H. and Schrag, D. (2021) Diagnosis and treatment of metastatic colorectal cancer: a review. *JAMA* **325**, 669-685.

Braicu, C., Buse, M., Busuioc, C., Drula, R., Gulei, D., Raduly, L., Rusu, A., Irimie, A., Atanasov, A. G., Slaby, O., Ionescu, C. and Berindan-Neagoe, I. (2019) A comprehensive review on MAPK: a promising therapeutic target in cancer. *Cancers (Basel)* **11**, 1618.

Dalton, S. O., Mellemkjaer, L., Thomassen, L., Mortensen, P. B. and Johansen, C. (2005) Risk for cancer in a cohort of patients hospitalized for schizophrenia in Denmark, 1969-1993. *Schizophr. Res.* **75**, 315-324.

Dhillon, A. S., Hagan, S., Rath, O. and Kolch, W. (2007) MAP kinase signalling pathways in cancer. *Oncogene* **26**, 3279-3290.

Driver, J. A., Logroscino, G., Buring, J. E., Gaziano, J. M. and Kurth, T. (2007) A prospective cohort study of cancer incidence following the diagnosis of Parkinson's disease. *Cancer Epidemiol. Biomarkers Prev.* **16**, 1260-1265.

Fang, J. Y. and Richardson, B. C. (2005) The MAPK signalling pathways and colorectal cancer. *Lancet Oncol.* **6**, 322-327.

Gargalionis, A. N., Papavassiliou, K. A. and Papavassiliou, A. G. (2021) Targeting STAT3 signaling pathway in colorectal cancer. *Biomedicines* **9**, 1016.

Gholipour, N., Ohradanova-Repic, A. and Ahangari, G. (2018) A novel report of MiR-4301 induces cell apoptosis by negatively regulating DRD2 expression in human breast cancer cells. *J. Cell. Biochem.* **119**, 6408-6417.

Gkouveris, I., Nikitakis, N., Karanikou, M., Rassidakis, G. and Sklavounou, A. (2014) Erk1/2 activation and modulation of STAT3 signaling in oral cancer. *Oncol. Rep.* **32**, 2175-2182.

Jan, R. and Chaudhry, G. E. (2019) Understanding apoptosis and apoptotic pathways targeted cancer therapeutics. *Adv. Pharm. Bull.* **9**, 205-218.

Kahsai, A. W., Shah, K. S., Shim, P. J., Lee, M. A., Shreiber, B. N., Schwalb, A. M., Zhang, X., Kwon, H. Y., Huang, L. Y., Soderblom, E. J., Ahn, S. and Lefkowitz, R. J. (2023) Signal transduction at GPCRs: allosteric activation of the ERK MAPK by beta-arrestin. *Proc. Natl. Acad. Sci. U. S. A.* **120**, e2303794120.

Kim, K., Han, Y., Duan, L. and Chung, K. Y. (2022) Scaffolding of mitogen-activated protein kinase signaling by beta-arrestins. *Int. J. Mol. Sci.* **23**, 1000.

Kundu, J., Choi, B. Y., Jeong, C. H., Kundu, J. K. and Chun, K. S. (2014) Thymoquinone induces apoptosis in human colon cancer HCT116 cells through inactivation of STAT3 by blocking JAK2- and Src-mediated phosphorylation of EGF receptor tyrosine kinase. *Oncol. Rep.* **32**, 821-828.

Mengie Ayele, T., Tilahun Muche, Z., Behaile Teklemariam, A., Bogale Kassie, A. and Chekol Abebe, E. (2022) Role of JAK2/STAT3 signaling pathway in the tumorigenesis, chemotherapy resistance, and treatment of solid tumors: a systemic review. *J. Inflamm. Res.* **15**, 1349-1364.

Midthun, L., Shaheen, S., Deisch, J., Senthil, M., Tsai, J. and Hsueh, C. T. (2019) Concomitant KRAS and BRAF mutations in colorectal cancer. *J. Gastrointest. Oncol.* **10**, 577-581.

Mu, J., Huang, W., Tan, Z., Li, M., Zhang, L., Ding, Q., Wu, X., Lu, J., Liu, Y., Dong, Q. and Xu, H. (2017) Dopamine receptor D2 is correlated with gastric cancer prognosis. *Oncol. Lett.* **13**, 1223-1227.

Oh, H. J., Magar, T. B. T., Pun, N. T., Lee, Y., Kim, E. H., Lee, E. S. and Park, P. H. (2018) YJI-7 suppresses ROS production and expression of inflammatory mediators via modulation of p38MAPK and JNK signaling in RAW 264.7 macrophages. *Biomol. Ther. (Seoul)* **26**, 191-200.

Park, K. H., Joo, S. H., Seo, J. H., Kim, J., Yoon, G., Jeon, Y. J., Lee, M. H., Chae, J. I., Kim, W. K. and Shim, J. H. (2022) Licochalcone H induces cell cycle arrest and apoptosis in human skin cancer cells by modulating JAK2/STAT3 signaling. *Biomol. Ther. (Seoul)* **30**, 72-79.

Perillo, B., Di Donato, M., Pezone, A., Di Zazzo, E., Giovannelli, P., Galasso, G., Castoria, G. and Migliaccio, A. (2020) ROS in cancer therapy: the bright side of the moon. *Exp. Mol. Med.* **52**, 192-203.

Piao, M. J., Han, X., Kang, K. A., Fernando, P., Herath, H. and Hyun, J. W. (2022) The endoplasmic reticulum stress response mediates shikonin-induced apoptosis of 5-fluorouracil-resistant colorectal cancer cells. *Biomol. Ther. (Seoul)* **30**, 265-273.

Pierce, S. R., Fang, Z., Yin, Y., West, L., Asher, M., Hao, T., Zhang, X., Tucker, K., Staley, A., Fan, Y., Sun, W., Moore, D. T., Xu, C., Tsai, Y. H., Parker, J., Prabhu, V. V., Allen, J. E., Lee, D., Zhou, C. and Bae-Jump, V. (2021) Targeting dopamine receptor D2 as a novel therapeutic strategy in endometrial cancer. *J. Exp. Clin. Cancer Res.* **40**, 61.

Ponsioen, B., Post, J. B., Buissant des Amorie, J. R., Laskaris, D., van Ineveld, R. L., Kersten, S., Bertotti, A., Sassi, F., Sipieter, F., Cappe, B., Mertens, S., Verlaan-Klink, I., Boj, S. F., Vries, R. G. J., Rehmann, H., Vandenabeele, P., Riquet, F. B., Trusolino, L., Bos, J. L. and Snippert, H. J. G. (2021) Quantifying single-cell ERK dynamics in colorectal cancer organoids reveals EGFR as an amplifier of oncogenic MAPK pathway signalling. *Nat. Cell Biol.* **23**, 377-390.

Qu, C., Park, J. Y., Yun, M. W., He, Q. T., Yang, F., Kim, K., Ham, D., Li, R. R., Iverson, T. M., Gurevich, V. V., Sun, J. P. and Chung, K. Y. (2021) Scaffolding mechanism of arrestin-2 in the cRaf/MEK1/ERK signaling cascade. *Proc. Natl. Acad. Sci. U. S. A.* **118**, e2026491118.

Raut, P. K. and Park, P. H. (2020) Globular adiponectin antagonizes leptin-induced growth of cancer cells by modulating inflammasomes activation: critical role of HO-1 signaling. *Biochem. Pharmacol.* **180**, 114186.

Raut, P. K., Lee, H. S., Joo, S. H. and Chun, K. S. (2021) Thymoquinone induces oxidative stress-mediated apoptosis through down-regulation of Jak2/STAT3 signaling pathway in human melanoma cells. *Food Chem. Toxicol.* **157**, 112604.

Richa, S., Dey, P., Park, C., Yang, J., Son, J. Y., Park, J. H., Lee, S. H., Ahn, M. Y., Kim, I. S., Moon, H. R. and Kim, H. S. (2020) A new histone deacetylase inhibitor, MHY4381, induces apoptosis via generation of reactive oxygen species in human prostate cancer cells. *Biomol. Ther. (Seoul)* **28**, 184-194.

Sahin, I. H., Ciombor, K. K., Diaz, L. A., Yu, J. and Kim, R. (2022) Immunotherapy for microsatellite stable colorectal cancers: challenges and novel therapeutic avenues. *Am. Soc. Clin. Oncol. Educ. Book* **42**, 1-12.

Shakya, R., Byun, M. R., Joo, S. H., Chun, K. S. and Choi, J. S. (2023) Domperidone exerts antitumor activity in triple-negative breast cancer cells by modulating reactive oxygen species and JAK/STAT3 signaling. *Biomol. Ther. (Seoul)* **31**, 692-699.

Wang, C. and Youle, R. J. (2009) The role of mitochondria in apoptosis. *Annu. Rev. Genet.* **43**, 95-118.